

Article

Not peer-reviewed version

Facile Synthesis Monodisperse SiO₂ Sphere And Their Application Performances in Chemical Mechanical Polishing

[Jinlong Ge](#)^{*}, Lingli Liu, [Xiaoqi Jin](#), Liyuan Zhang, Yuhong Jiao, Qiuqin Wang, Yongkui Wang

Posted Date: 15 August 2023

doi: 10.20944/preprints202308.0655.v2

Keywords: Stöber method; SiO₂ sphere; chemical mechanical polishing; SiO₂ slurry



Preprints.org is a free multidiscipline platform providing preprint service that is dedicated to making early versions of research outputs permanently available and citable. Preprints posted at Preprints.org appear in Web of Science, Crossref, Google Scholar, Scilit, Europe PMC.

Copyright: This is an open access article distributed under the Creative Commons Attribution License which permits unrestricted use, distribution, and reproduction in any medium, provided the original work is properly cited.

Article

Facile Synthesis Monodisperse SiO₂ Sphere and Their Application Performances in Chemical Mechanical Polishing

Jinlong Ge^{1,2,*}, Lingli Liu³, Xiaoqi Jin^{1,2}, Liyuan Zhang^{1,2}, Yuhong Jiao^{1,2}, Qiuqin Wang^{1,2} and Yongkui Wang^{1,2}

¹ School of Materials and Chemical Engineering, Bengbu University, Bengbu 233030, China

² Anhui Provincial Engineering Laboratory of Silicon-Based Materials, Bengbu University, Bengbu 233030, China

³ School of Energy, Materials and Chemical Engineering, Hefei University, Hefei, China

* Correspondence: jinlongge2005@126.com

Abstract: The chemical mechanical polishing (CMP) has been widely used for surface modification of critical materials and components and provided global planarization of topography with a low post-planarization slope high quality and efficiency. The colloidal silica slurries play an important role in the finishing processes of optical components. Monodisperse mesoporous silica nanospheres were synthesized with different surfactant by Stöber method. Their architectural features and texture parameters were characterized by XRD, FTIR, N₂ adsorption-desorption isotherms, SEM, XPS, and TGA techniques. The spherical SiO₂ products presented with the controllable 50-150 nm particle size and distribution. The AFM micrographs reveal that flat and smooth surfaces without distinct scratches residual particles are achieved by using the as-obtained composite particles as abrasives. The particle size of SiO₂ slurry plays a critical role in the chemical-mechanical polishing process.

Keywords: Stöber method ;SiO₂ sphere; chemical mechanical polishing; planarization; SiO₂ slurry

1. Introduction

Chemical mechanical polishing (CMP) is an essential technology to improve the atomic-level planarization of a diverse variety of materials, such as silicon wafers, silicon carbide, sapphire, copper, gallium nitride, and glass[1–3]. In a typical CMP process, there are many influencing factors involved in polishing planarization process including pad properties, slurry characteristics and processing conditions. It is well known that chemical and mechanical mechanisms are two important mechanisms in polishing process[4–6]. Investigations of the variables in the CMP process, solid loading, particle size and distribution, modulus, hardness, asperity sizes and distribution, down-pressure, velocity are believed to be responsible for the material removal[7–9]. It is essential to develop a novel green slurry to perform CMP for sapphire wafers used for high performance devices, eliminating the environmental contamination and reducing potential harmful impact on operators[10]. The physicochemical properties of abrasives play a critically important role in the performance of silicon wafers[11–13].

Currently, the mechanically active silica (SiO₂), ceria (CeO₂), alumina (Al₂O₃) [14], zirconia (ZrO₂) are widely used in preparation of abrasives[15]. Novel environment-friendly silica slurries have been developed[16]. The silica slurries provide high polishing rate, good planarity, and high selectivity, which have greatest influence and play an important role in the optimization of the CMP process. The regular ball like shapes SiO₂ abrasives have less scratches damage or defects during CMP[17–19].

Substantial research efforts have been made to improve the MRR of The silicon wafers with minimally damaged surfaces during the CMP process using silica abrasives[20–22]. Chen et al. estimated the interaction forces between the substrate surfaces and the abrasive nanoparticles, the ceria particle processed a chemical tooth and formed Si-O-Ce bonds between ceria particles and the

sample surface[23]. Chen et al. prepared parallel channels hexagonal mesoporous silica (H-mSiO₂) particles, which attached with CeO₂ nanoparticles. The H-mSiO₂-CeO₂ composite particles as abrasives revealed a reduced surface roughness, a low topographical variation, and an improved removal rate. Shi et al. reported on a novel acid based SiO₂ slurry which can simultaneously realize an ultralow R_q of only ~0.193 nm and a high MRR of ~10.9 μm h⁻¹ on the FS substrate. Chen et al. used the good uniformity and dispersity 30-140 nm D-mSiO₂ nanospheres as functionalized abrasives[24]. The abrasives played a key role and achieve nearly non-damage surfaces with atomic level roughness, which can avoid surface scratches commonly caused by particle agglomerations in slurries[25].

In this work, we successfully synthesized monodispersed SiO₂ nanospheres by Stöber method with the controllable 50-150 nm particle size and distribution. Furthermore, the CMP performance using silica colloid with different sizes have been studied. In addition, the possible CMP mechanism of the developed polishing slurry containing SiO₂ with different sizes abrasives wafers was proposed.

2. Experimental Section

2.1. Materials

Tetraethylorthosilicate (TEOS, A.R.), ammonia aqueous solution (28 wt%), Ethanol (A.R.), Cetyltrimethylammonium chloride(CTAC, A.R.), Cetyltrimethylammonium bromide (CTAB, A.R.), Octadecyltrimethyl ammonium bromide (STAB, A.R.), Cetyldimethyl benzyl ammonium chloride (HDBAC, A.R.), Triethanolamine (TEA, A.R.), NH₄F, NaOH, Ethanol were purchased from Sinopharm Chemical Reagent Co., Ltd. All chemicals were used as received without further purification. Deionized water was used in all experiments.

2.2. Preparation of silica spheres

Silica spheres were synthesized by the Stöber method[26]. Typically, Solution A: a combination of 100 mg NH₄F (2.7 mmol), 21.7 g H₂O (1.12 mol) and 2.41 mL of a 25% aqueous CTAC solution (1.83 mmol) was stirred at 750 rpm in a 50 mL round bottom flask equipped with a stir bar and heated to 60°C. Solution B: 14.35 g TEA (97 mmol) and 2.06 mL TEOS (9.3 mmol) were statically heated in a 20 mL capped polypropylene vial at 90°C for 30 minutes. Both components remain unmixed after heating. Solution B was then added to solution A at once while stirring vigorously, followed by removal of the oil bath, leaving the reaction solution to slowly cool down to room temperature while continuing to stir overnight. On the next day after 12 hours, 50 mL ethanol was added to the solution, which was then transferred into two 50 mL centrifuge tubes and spun down at a speed of 20000 rpm for 20 minutes at room temperature. The supernatant of the solutions was decanted, and the samples were refilled with 30 mL ethanol each, redispersed mechanically with a spatula and by sonication for 10 minutes, and centrifuged again[27]. The sample was named CTAC-SiO₂. The CTAB-SiO₂, STAB-SiO₂, HDBAC-SiO₂ were synthesized analogously by replacing CTAC with the equivalent molar amounts of CTAB, STAB, HDBAC, respectively.

2.4. Polishing tests and evaluations

CMP experiments on silicon wafers were performed on a UNIPOL-300 CMP machine (Shenyang Kejing Instrument Co., Ltd., China) with a Rodel porous polyurethane pad. The force-volume images were recorded with the resolution typically of 10×10 pixels within a scanning area of 3×3 μm² area. The 1 wt% solid content SiO₂ abrasive particles were dispersed into deionized water and treated by sonication for 30 min before use. And the slurry pH values were adjusted to 8.5-8.6 using 0.1 M NaOH solution. The polishing parameters were: the feed rate of the polishing liquid was 180 ml/min, the pressure and table-platen speed are fixed at 6 psi and 70 rpm, and the polishing time was 2 h. After polishing, the substrates were cleaned with ultrasonic in DI water. Finally, they were dried with a stream of nitrogen prior to surface analyses.

2.3. Characterization

Fourier transform infrared spectra (FT-IR) were measured using KBr pellets on a Nicolet iS10 analyzer using a scanned area of $4000\text{--}400\text{ cm}^{-1}$ and a 4 cm^{-1} resolution. The samples were treated using the potassium bromide pellet technique before testing. The crystal structures of the samples were characterized by powder X-ray diffraction on a Rigaku SmartLab SE with Cu K α radiation ($\lambda=1.54056\text{ \AA}$). The diffraction data were collected over the angle range of $5\text{--}80^\circ$ with a step size of 0.02 at 35 kV and 20 mA. Thermogravimetric Analysis was performed on an in the temperature range of $30\text{--}900^\circ\text{C}$ under nitrogen at a heating rate of 10°Cmin^{-1} with a Netzsch STA 2500 Regulus analyzer. Nitrogen sorption desorption isotherms were obtained at 77 K using a Micromeritics ASAP 2020 sorptionmeter. The surface area based on the N $_2$ isotherm data was analyzed by BET (Brunauer–Emment–Teller). The elemental composition of the surfaces was determined with a Kratos Analytical Axis Ultra X-ray photoelectron spectrometer equipped with a monochromatic Al K α source. The structure and morphology of samples were investigated with Zeiss Sigma 300 scanning electron microscopy at an acceleration voltage of 15 kVa. Surface roughness and surface morphology of the polished silicon wafers were characterized by Atomic Force Microscopy with Multimode 8, Bruker, Santa Barbara, CA.

3. Results and Discussion

3.1. Structural and Textural Features

The XRD patterns of the SiO $_2$ sample were measured and were showed in Figure 1. As can be seen, the strong and broad diffraction peak at 2θ of 23° in good agreement with the positions of pure amorphous silica[28]. This result means that no discernible long-range order in the pore arrangement exists in the SiO $_2$. These observations illustrated that the silica microsphere were successfully synthesized using the sol-gel method.

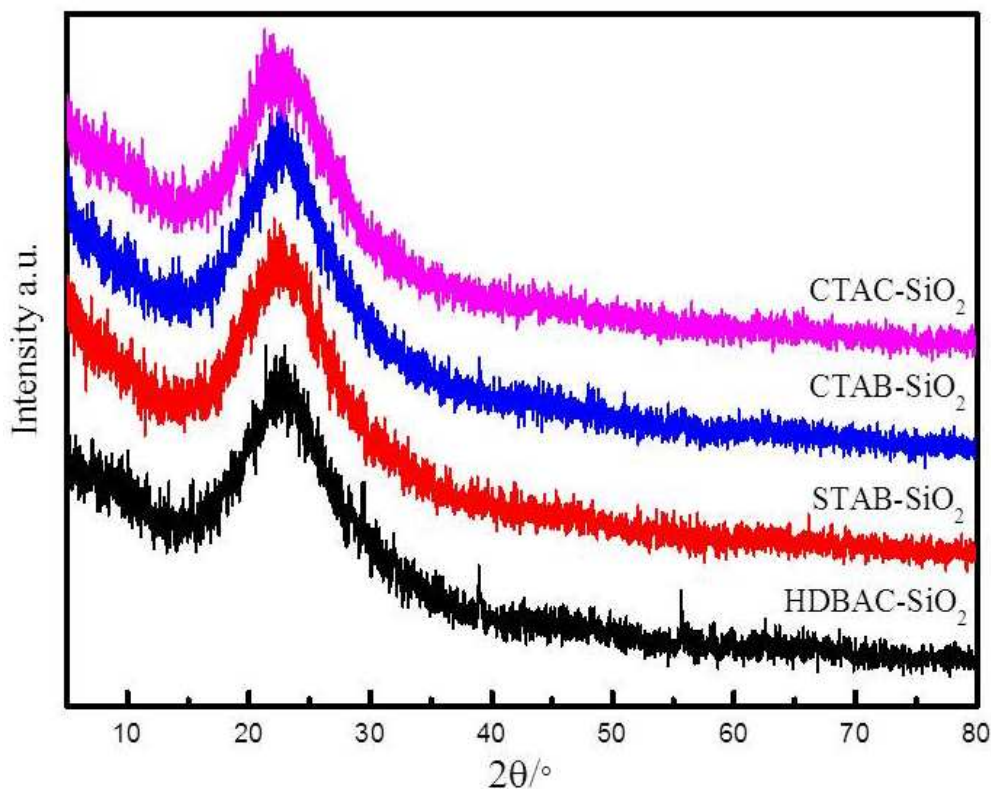


Figure 1. XRD patterns of SiO $_2$ microsphere.

The composition of silica spheres was established by FT-IR spectrum as shown in Figure 2. The strong band at 3442.2 cm^{-1} can be ascribed to the absorption of -OH group of silica spheres. The absorption band appears at 2983.39 cm^{-1} indicated that the stretching vibration of -CH₃ in the CTAB. The peak at 1630.5 cm^{-1} can be attributed to the bending vibration of H₂O. The peak with a wavenumber of 1404.9 and 1383.8 cm^{-1} belongs to the -CH₃ and -CH₂ symmetric bending vibrations, respectively. The peak at 970.9 cm^{-1} is associated with the bending vibration of Si-OH. The obvious bands located at 1054.7 and 457 cm^{-1} can be assigned to the stretch vibration bands of Si-O-Si bond, respectively [29]. It indicates that SiO₂ is hydrophilic and there are many hydroxyl groups on the surface of it.

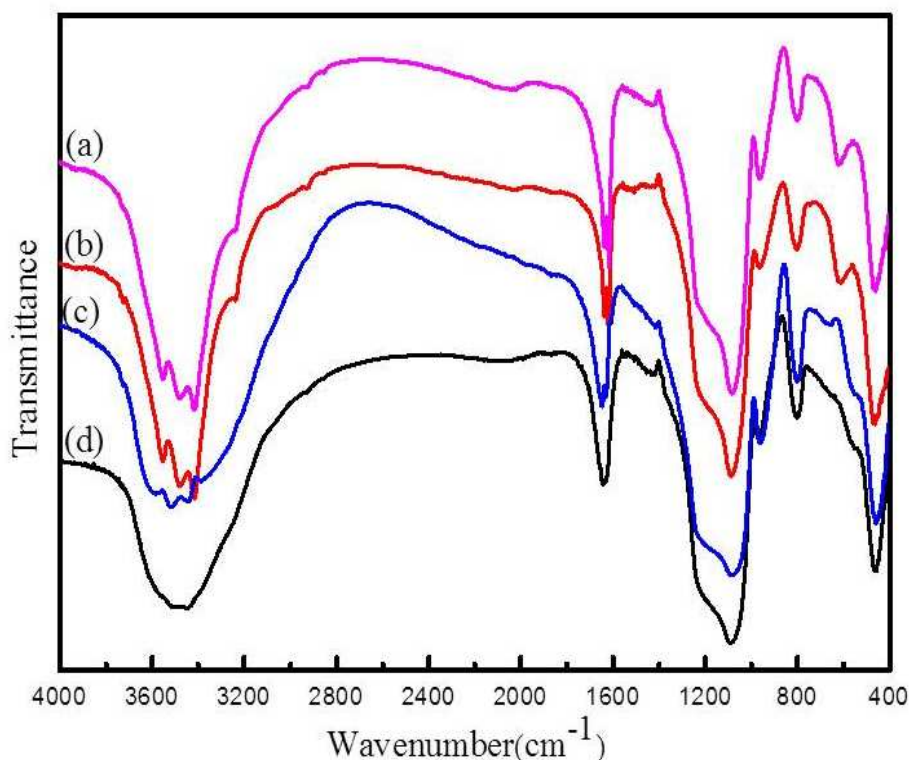


Figure 2. FTIR spectra of SiO₂ microsphere. (a) CTAC-SiO₂, (b) CTAB-SiO₂, (c) STAB-SiO₂, (d) HDBAC-SiO₂.

The TGA curves of SiO₂ from different preparation conditions are given in Figure 3. The first slight weight loss of 8% below 120°C is attributed to the dissociation of the absorbed water. The second weight loss of 15% between 120°C to 550°C can be attributed to the degradation of organic parts [30].

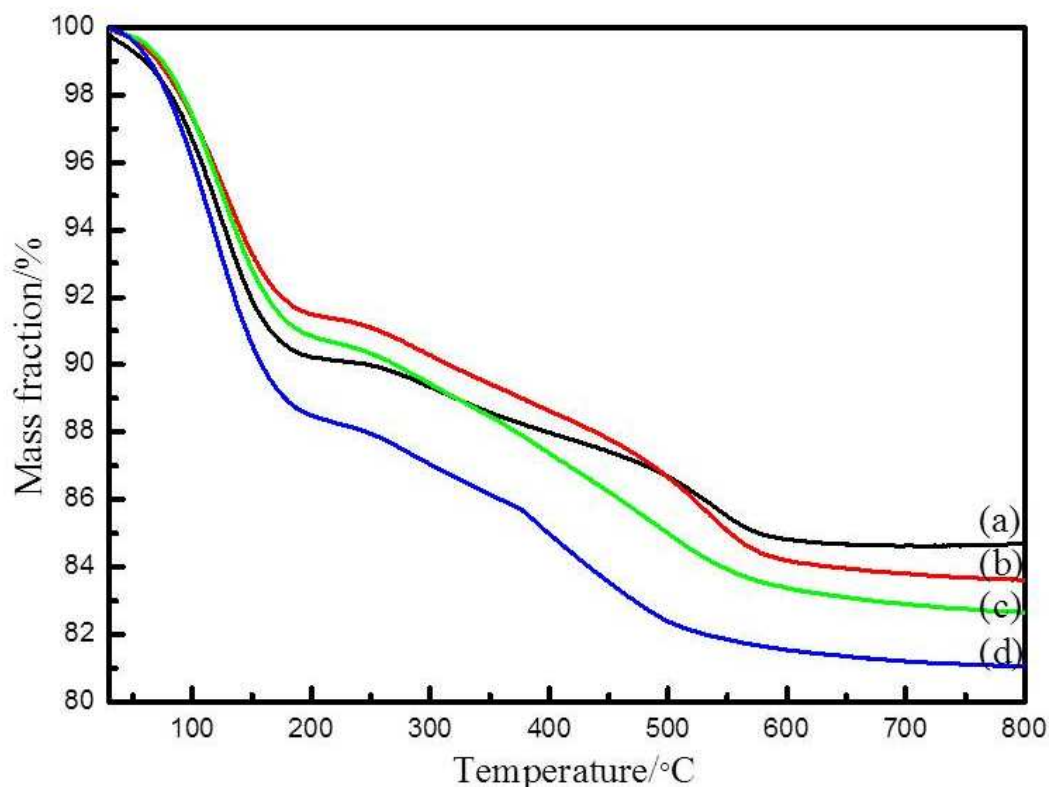


Figure 3. TGA spectra of SiO₂ microsphere. (a) CTAC-SiO₂, (b) CTAB-SiO₂, (c) STAB-SiO₂, (d) HDBAC-SiO₂.

The Brunauer-Emmett-Teller (BET) specific surface area during the synthesis of silica spheres were monitored by the nitrogen adsorption-desorption isotherms (Figure 4). The adsorption isotherms of silica spheres show a typical type IV adsorption isotherm, which is normally attributed to the characteristics of ordered mesoporous channels. The sorption shows a pore-condensation step around the relative pressure range $p/p_0 = 0.3-0.4$. Specifically, the BET surface areas of CTAC-SiO₂, CTAB-SiO₂, STAB-SiO₂, and HDBAC-SiO₂ were comparably decreased from 1155.9, 1059.0, and 1119.2 to 796.9 m²g⁻¹. The pore size of these samples was reduced from 2.4, 2.4, and 2.38 to 2.35 nm. The pore size did not change significantly.

Table 1. The structure parameters of all related samples.

Samples.	S _{BET} (m ² g ⁻¹)	Pore size (nm)
CTAC-SiO ₂	1155.9	2.40
CTAB-SiO ₂	1119.2	2.40
STAB-SiO ₂	1059.0	2.38
HDBAC-SiO ₂	796.9	2.35

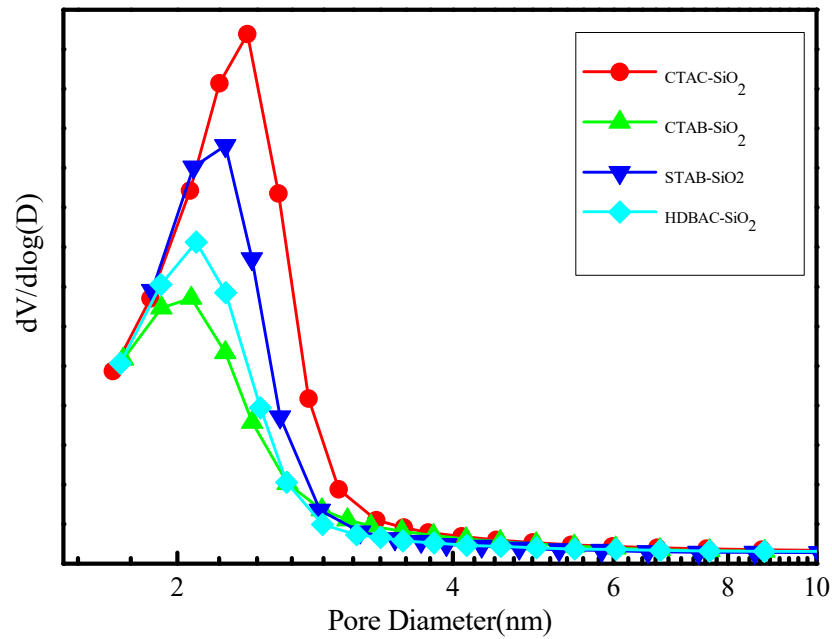


Figure 4. The corresponding pore size distributions.

The particle size and morphology of SiO₂ microspheres were confirmed by SEM, as shown in Figure 5. All samples have a regular spherical shape[31]. The surface of CTAB-SiO₂ and CTAC-SiO₂ are smoother than that of other surfactants-SiO₂. The average particle sizes of SiO₂ microspheres samples are ca. 30 nm-150 nm, respectively.

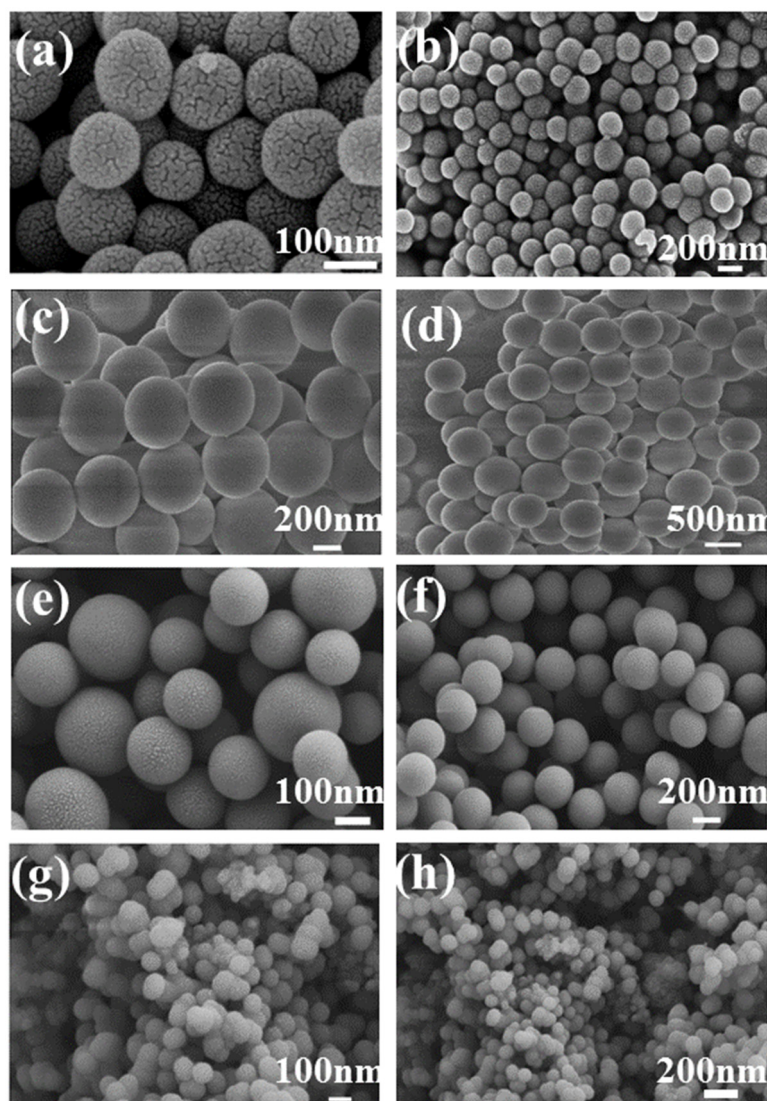


Figure 5. SEM images. (a)(b) CTAC-SiO₂,(c) (d)CTAB-SiO₂,(e) (f) STAB-SiO₂,(g) (h) HDBAC-SiO₂.

The X-ray photoelectron spectroscopy (XPS) is a highly sensitive technique to explore the chemical changes in the element surroundings. The XPS spectra of the elements of Si2p, O1s and C1s are shown in Figure 6. The spectrum of SiO₂ microspheres shows strong peaks at 531.9 eV corresponding to the binding energy of O1s[32,33]. The spectrum at the BE of 533.19 eV and 532.94 eV, corresponding to Si-O. The electronic binding energy of C1s peak at 284.6 eV was corresponded to C-C bonding[34]. The peaks at 283.4 and 286.3 eV corresponded to C-Si and H-C bonding. The peaks of 103.75 and 103.9 eV were assigned to Si2p. The small shoulder peak of 102.9 eV was reported to H₆C₂Si₂O₃. Slurry actively reacts with the oxide surface leading dissolution of Si-O bonds to H-C-O-Si bonds[35]. This hydro-carbonated surface of oxide film was easier to be removed by mechanical parts of CMP process.

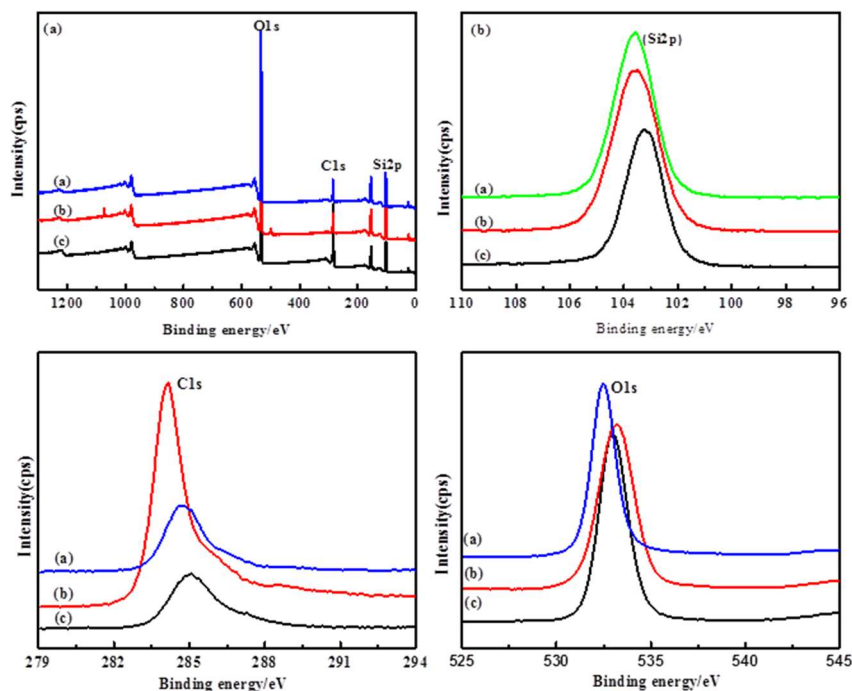


Figure 6. XPS spectra of SiO_2 microsphere. (a) CTAC- SiO_2 , (b) CTAB- SiO_2 , (c) STAB- SiO_2 .

3.2. Polishing performance of SiO_2 microsphere

The surface quality of polished silicon wafers after polishing with CTAB- SiO_2 , CTAC- SiO_2 , STAB- SiO_2 and HDBAC- SiO_2 particles can be investigated through their surface topographies, which were achieved by AFM optical microscope. As shown in Figure 7, the AFM micrographs reveal that flat and smooth surfaces without distinct scratches residual particles are achieved by using the as-obtained composite particles as abrasives[36,37]. The scratches as well as other microdefects could hardly be observed[38,39]. The silica abrasive particle size plays an essential role during CMP process. It is clearly seen that CTAB- SiO_2 , CTAC- SiO_2 abrasives have much more regular round shapes and remain independent for each particle[40,41]. There are some mechanical scratches and cracks are distributed deeply on HDBAC- SiO_2 abrasives. The HDBAC- SiO_2 particle size were about 140 nm, which was larger than the other there SiO_2 abrasives[42,43]. The surfactants group may be adsorbed on the surface of SiO_2 abrasive under the action of electrostatic attraction. The Si-OH in the slurry interacts with the silicon wafer surface in a similar fashion to the Si-OH on the SiO_2 grain surface, both in the form of bridge bonds to reduce the breakage bond energy of the Si-Si bonds inside the silicon[44,45]. It is noteworthy that the optimal polishing performance can be achieved by controlling the balance between the chemical effect and the mechanical effect[46].

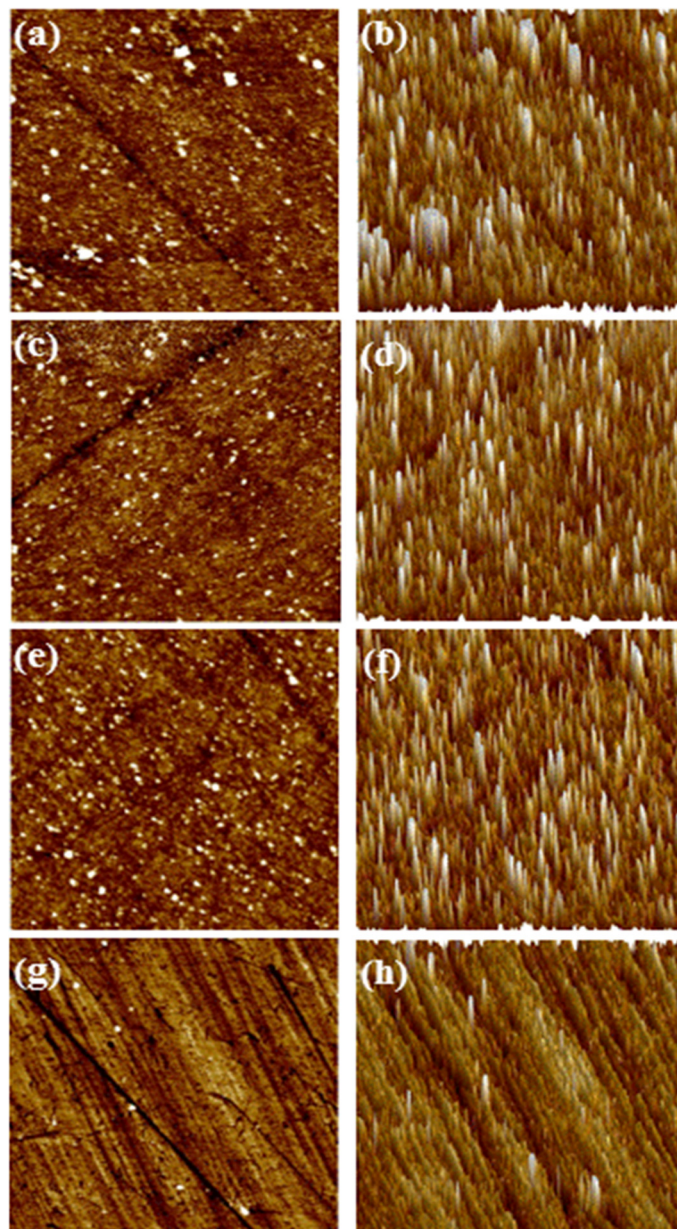


Figure 7. AFM images of the surfaces after CMP with SiO₂ microsphere. (a)(b) CTAC-SiO₂,(c) (d)CTAB-SiO₂,(e) (f) STAB-SiO₂,(g) (h) HDBAC-SiO₂.

4. Conclusions

In summary, the controllable 50-150 nm sizes SiO₂ microsphere were successfully synthesized by the Stöber method with a series of cationic surfactants. The spherical SiO₂ exhibited an improved surface quality in the chemical-mechanical polishing process. The polishing results indicate that the SiO₂ abrasives can achieve a substantial improvement of surface planarization. The novel SiO₂ abrasives were successful applications in CMP.

Author Contributions: J.G. carried the main responsibility for the writing of the manuscript. X.J. supervised the preparation work and contributed to writing the manuscript. L.Z., Y.J.,Q.W. Y.W. assisted J. G. carried out the synthesized and characterized experiment. J. G. was responsible for analyzing the obtained data. All authors have read and agreed to the published version of the manuscript.

Funding: This work was supported by the top notch talent grants programme from Anhui Provincial Education Department , China (Grant No. gxbjZD2020092) ; The excellent innovative scientific research team of silicon-based materials (2022AH010101) ;The Major Research Project of Natural Science from the Anhui Provincial Education Department , China (Grant No. KJ2019ZD62, No. KJ2021ZD0140); The key research and development

project of Anhui Province (Grant No. 202004a05020017); The high-level scientific research and cultivation projects of Bengbu University (Grant No. 2021pyxm09, 2021pyxm08).

Acknowledgments: We extend our appreciation to Anhui Province Engineering Laboratory of Silicon-based Materials; Functional Powder Material Lab of Bengbu City; Engineering Technology Research Center of Silicon-based Materials, Anhui Provincial for funding this work.

Conflicts of Interest: The authors declare no conflict of interest.

References

1. Lu, Z.y.; Ryde, N.P.; Babu, S. V.; Matijevi,E. Particle adhesion studies relevant to chemical mechanical polishing. *Langmuir*. **2005**, 21, 22, 9866-9872
2. Wang, H.Q.; Xu, Z.J.; Fink, M.J.; Shchukina, D.; Mitchell B.S. Functionalized silicon nanoparticles from reactive cavitation erosion of silicon wafers. *Chem. Commun.*, 2015, 51, 1465-1468
3. Shi, X.L.; G.P. Chen.; Xua, L.; Kang, C.X.; Luo, G.H.; Zhou, Y.; Dargusch, M. S.; Pan, G.S. Achieving ultralow surface roughness and high material removal rate in fused silica via a novel acid SiO₂ slurry and its chemical-mechanical polishing mechanism. *Appl.Surf.Sci.* **2020**, 500, 144041-144049
4. Stavreva, Z.; Zeidler, D.; Plotner, M.; Drescher, K. Characteristics in chemical mechanical polishing of copper: comparison of polishing pads. *Appl.Surf.Sci.* **1997**, 108, 39-44
5. Kawaguchi, K.; Wang, Y.; Xu, J.X.; Ootani, Y.; Higuchi, Y.J.; Ozawa, N.; Kubo, Mo. Atom-by-atom and sheet-by-sheet chemical mechanical polishing of diamond assisted by OH radicals: a tight-binding quantum chemical molecular dynamics simulation study. *ACS Appl.Mater.Inter.* **2021**, 13, 41231-41237
6. Luo, Q.; Mackay, R. A.; Babu, S. V. Copper dissolution in aqueous ammonia containing media during chemical mechanical polishing. *Chem.Mater.* **1997**, 9, 10, 2101-2106
7. Penta, N. K.; Veera, P. R. D.; Babu, S. V. Role of poly(diallyldimethylammonium chloride) in selective polishing of polysilicon over silicon dioxide and silicon nitride films. *Langmuir*. **2011**, 27, 7, 3502-3510
8. Huang, C.J.; Mu, W.X.; Zhou, H.; Zhu, Y.W.; Xu, X.M.; Jia, Z.T.; Zheng, L.; Tao, X.T. Effect of OH⁻ on chemical mechanical polishing of β-Ga₂O₃ (100) substrate using an alkaline slurry. *RSC Adv.*, **2018**, 8, 6544-6550
9. Tseng, K.C.; Yen, Y.T.; Thomas, S.R.; Tsai, H.W.; Hsu, C.H.; Tsai, W.C.; Shen, C.H.; Shieh, J.M.; Wang, Z. M.; Chueh, Y.L. A facile chemical mechanical polishing lift off transfer process toward large scale Cu(In,Ga)Se₂ thin-film solar cells on arbitrary substrates. *Nanoscale*, **2016**, 8, 5181-5188
10. He, J.; Li, X.L.; Su, D.; Ji, H.M.; Zhang, X.; Zhang, W.S. Super hydrophobic hexamethyl disilazane modified ZrO₂-SiO₂ aerogels with excellent thermal stability. *J. Mater. Chem. A*, **2016**, 4, 5632-5638
11. Luo, J.F.; Dornfeld, D.A. Material removal mechanism in chemical mechanical polishing: theory and modeling. *IEEE Trans. Semicon. Manufa.* 2001. 14, 2, 112-133
12. Luo, Q.; Mackay, R. A.; Babu, S. V. Copper dissolution in aqueous ammonia containing media during chemical mechanical polishing[J]. *Chem.Mater.* **1997**, 9, 10, 2101-2106
13. Miller, M.S.; Ferrato, M.A.; Niec, A.; Biesinger, M. C.; Carmichael, T.B. Ultrasoother gold surfaces prepared by chemical mechanical polishing for applications in nanoscience. *Langmuir*. **2014**, 30, 47, 14171-14178
14. Wen, J.L.; Ma, T.B.; Zhang, W.W.; Duin, A.C.; Lu, X.C. Surface orientation and temperature effects on the interaction of silicon with water: molecular dynamics simulations using reaxFF reactive force field. *J.Phys.Chem.A*. **2017**, 121, 3, 587-594
15. Dobbs, H.A.; Degen, G.D.; Berkson, Z.J.; Kristiansen, K.; Schrader, A.M.; Oey, T.; Sant, G.C.; Israelachvili, J.N. Electrochemically enhanced dissolution of silica and alumina in alkaline environments. *Langmuir*. **2019**, 35, 48, 15651-15660
16. Yang, X.; Sun, R.Y.; Kawai, K.; Arima, K.; Yamamura, K. Surface modification and microstructuring of 4H-SiC(0001) by anodic oxidation with sodium chloride aqueous solution. *ACS Appl.Mater.Inter.* **2019**, 11, 2, 2535-2542
17. Wang, Y.G.; Chen, Y.; Qi, F.; Zhao, D.; Liu, W.W. A material removal model for silicon oxide layers in chemical mechanical planarization considering the promoted chemical reaction by the down pressure. *Tribol. Int.* **2016**, 93, 11-16.
18. Xu, L.; Lei, H.; Wang, T. X.; Dong, Y.; Dai, S.W. Preparation of flower-shaped silica abrasives by double system template method and its effect on polishing performance of sapphire wafers. *Ceram.Int.* **2019**, 45, 7, 8471-8476
19. Lei, H.; Luo, J.B. CMP of hard disk substrate using a colloidal SiO₂ slurry: preliminary experimental investigation. *Wear*, **2004**, 257, 461-470
20. Kim, R.; Sung, Y. I.; Lee, J. S.; Lim, H. B. Chemiluminescence system for direct determination and mapping of ultra-trace metal impurities on a silicon wafer. *Analyst*, **2010**, 135, 2901-2906

21. Zhou, Y.; Pan, G.S.; Gong, H.; Shi, X.L. Characterization of sapphire chemical mechanical polishing performances using silica with different sizes and their removal mechanisms. *Colloid. Surf. A.* **2017**, 513, 153-159
22. Lv, M.X.; Yu, S.T.; Liu, S.W.; Li, L.; Yu, H.H.; Wu, Q.; Pang, J.H.; Liu, Y.X.; Xie, C.X.; Liu, Y. One-pot synthesis of stable Pd@mSiO₂ core-shell nanospheres with controlled pore structure and their application to the hydrogenation reaction. *Dalton Trans.*, **2019**, 48, 7015-7024
23. Chen, A.; Wang, S.R.; Cai, W.J.; Mu, Z.Y.; Chen, Y. Tunable synthesis, characterization, and CMP performance of dendritic mesoporous silica nanospheres as functionalized abrasives. *Colloid. Surface A.* **2022**, 638, 128322-128335
24. Chen, A.; Wang, W.Y.; Ma, X.Y.; Chen, Y. Ceria coated hexagonal mesoporous silica core shell composite particle abrasives for improved chemical mechanical planarization performance. *J. Porous Mater.* **2019**, 26 (4), 1005-1015
25. Ng, H.T.; Han, J.; Yamada, T.; Nguyen, P.; Chen, Y. P.; Meyyappan, M. Single crystal nanowire vertical surround gate field effect transistor. *Nano. Lett.* **2004**, 4, 7, 1247-1252
26. Stöber, W.; Fink, A.; Bohn, E. Controlled growth of monodisperse silica spheres in the micron size range. *J. Colloid Interface Sci.* **1968**, 26, 62-69.
27. Möller, K.; Bein, T. Talented mesoporous silica nanoparticles. *Chem. Mater.* **2017**, 29, 1, 371-388
28. Yoo, W.C.; Stein, A. Solvent effects on morphologies of mesoporous silica spheres prepared by pseudomorphic transformations. *Chem. Mater.* **2011**, 23, 1761-1767
29. Xie, W.X.; Zhang, Z.Y.; Liao, L.X.; Liu, J.; Su, H.J.; Wang, S.D.; Guo, D.M. Green chemical mechanical polishing of sapphire wafers using a novel slurry. *Nanoscale*, **2020**, 12, 22518-22526
30. Pan, G.S.; Gu, Z.H.; Zhou, Y.; Li, T.; Gong, H.; Liu, Y. Preparation of silane modified SiO₂ abrasive particles and their chemical mechanical polishing (CMP) performances. *Wear.* **2011**, 273, 100-104
31. Ryu, J.; Kim, W.; Yun, J.; Lee, K.; Lee, J.; Yu, H.; Kim, J.H.; Kim, J.J.; Jang, J. Fabrication of uniform wrinkled silica nanoparticles and their application to abrasives in chemical mechanical planarization. *ACS Appl. Mater. Interfaces.* **2018**, 10, 11843-11851
32. Zhang, L.; Wang, H.B.; Zhang, Z.F.; Qin, F.; Liu, W.L.; Song, Z.T. Preparation of monodisperse polystyrene/silica core-shell nano-composite abrasive with controllable size and its chemical mechanical polishing performance on copper. *Appl. Surf. Sci.* **2011**, 258, 1217-1224
33. Kim, N.H.; Ko, P.J.; Choi, G.W.; Seo, Y.J.; Lee, W.S. Chemical mechanical polishing (CMP) mechanisms of thermal SiO₂ film after high-temperature pad conditioning. *Thin Solid Films.* **2006**, 504, 166-169.
34. Myong, K.K.; Byun, J.; Choo, M.J.; Kim, H.; Kim, J.Y.; Lim, T.; Kim, J. Direct and quantitative study of ceria SiO₂ interaction depending on Ce³⁺ concentration for chemical mechanical planarization (CMP) cleaning. *Mat. Sci. Semicon. Proc.* **2021**, 122, 105500-105509
35. Chen, G.M.; Ni, Z.F.; Bai, Y.W.; Li, Q.Z.; Zhao, Y.W. The role of interactions between abrasive particles and the substrate surface in chemical-mechanical planarization of Si-face 6H-SiC. *RSC Adv.*, **2017**, 7, 16938-16952
36. Chen, Y.; Wei, A.L.; Ma, X.Y.; Wang, T.Y.; Chen, A. Copper incorporated dendritic mesoporous silica nanospheres and enhanced chemical mechanical polishing (CMP) performance via Cu²⁺/H₂O₂ heterogeneous Fenton-like system. *Appl. Surf. Sci.* **2022**, 601, 154262-154273
37. Matovu, J.B.; Ong, P.; Leunissen, L.H. A.; Krishnan, S.; Babu, S. V. Use of multifunctional carboxylic acids and hydrogen peroxide to improve surface quality and minimize phosphine evolution during chemical mechanical polishing of indium phosphide surfaces. *Ind. Eng. Chem. Res.* **2013**, 52, 10664-10672
38. Shi, X.L.; Xu, L.; Zhou, Y.; Zou, C.L.; Wang, R.R.; G.S. Pan. An in situ study of chemical mechanical polishing behaviours on sapphire (0001) via simulating the chemical product-removal process by AFM-tapping mode in both liquid and air environments. *Nanoscale.* **2018**, 10, 19692-19700
39. Myers, J.N.; Zhang, X.X.; Bielefeld, J.; Lin, Q.H.; Chen, Z. Nondestructive in situ characterization of molecular structures at the surface and buried interface of silicon supported low-k dielectric films. *J. Phys. Chem. B.* **2015**, 119, 4, 1736-1746
40. Wu, L.; Cui, L.C.; He, W.; Guo, J.; Yu, B.J.; Qian, L.M. Toward controllable wet etching of monocrystalline silicon: roles of mechanically driven defects. *ACS Appl. Mater. Interfaces.* **2022**, 14, 25, 29366-29376
41. Qin, K.; Moudgil, B.; Park, C.W. A chemical mechanical polishing model incorporating both the chemical and mechanical effects. *Thin Solid Films.* **2004**, 446, 277-286
42. Gao, P.L.; Liu, T.T.; Zhang, Z.Y.; Meng, F.N.; Ye, R.P.; Liu, J. Non-spherical abrasives with ordered mesoporous structures for chemical mechanical polishing. *Sci. China. Mater.* **2021**, 64, 11, 2747-2763
43. Wang, H.; Hu, L.J.; Cao, G.L.; Xia, R.Y.; Cao, J.W.; Zhang, J.L.; Pan, G.F. Experimental and computational studies on octyl hydroxamic acid as an environmentally friendly inhibitor of cobalt chemical mechanical polishing. *ACS Appl. Mater. Inter.* **2022**, 14, 24, 28321-28336

44. Zhang,Z.L.; Jin,Z.J.;J.Guo.The effect of the interface reaction mode on chemical mechanical polishing. *CIRPJ.Manuf.Sci.Tec.***2020**, 539-547
45. Bu,Z. Z.; Niu, F.L.; Chen, J.P.; Jiang, Z.L.; Wang,W.J.; Wang, X.H.; Wang, H.Q.; Zhang, Z.F.;Zhu,Y.W.;Sun,T.Single crystal silicon wafer polishing by pretreating pad adsorbing SiO₂ grains and abrasive-free slurries. *Mat.Sci.Semicon.Proc.* **2022**, 141,106418- 106427
46. Wang, M.; Duan,F.L.Atomic level material removal mechanisms of Si(110) chemical mechanical polishing: insights from ReaxFF reactive molecular dynamics simulations. *Langmuir.* **2021**, 37, 6, 2161-2169

Disclaimer/Publisher's Note: The statements, opinions and data contained in all publications are solely those of the individual author(s) and contributor(s) and not of MDPI and/or the editor(s). MDPI and/or the editor(s) disclaim responsibility for any injury to people or property resulting from any ideas, methods, instructions or products referred to in the content.